13th International Symposium on Particle Image Velocimetry – ISPIV 2019
Munich, Germany, July 22-24, 2019

Cold Flow Measurement in Optical Internal Combustion Engine using PIV

V. D. Tsiogkas*, A. Chraniotis, D. Kolokotronis, A. Tourlidakis

Department of Mechanical Engineering, University of Western Macedonia, Kozani, Greece

*vtsiogkas@uowm.gr

Abstract

Due to the upcoming legislation for the reduction vehicle greenhouse gases emissions, it is important to improve engine efficiency through the investigation of the flow field and the understanding of the turbulent mixing in order to partially replace the fossil fuels with renewable ones. Measurement of flow structures conducted using 2D digital Particle Image Velocimetry technique in a 475cc optical single – cylinder Gasoline Direct Injection (GDI) spark ignition engine. The experimental results include phase averaged flow fields during the intake stroke with 25% throttle position at 1000 and 1500 RPM. These sets of measurements were conducted for cold flow conditions at two different planes. The flow was recorded at 300, 260, and 220 crank angle degrees (CADs) before the combustion top dead center (BTDC). The spatial averaged TKE (Turbulent Kinetic Energy) was calculated along with the TR (Tumble Ratio). It was observed that a tumble like motion with Counter Clock Wise rotation (CCW) was present near the maximum valve lift timing of the intake valves. The peak TKE at the intake stroke was present at 260 CAD BTDC, for 1000RPM. The absolute value of TR, which corresponds to vorticity normalized by the angular velocity, was higher at 220 BTDC, 1500RPM at the tumble plane.

1. Introduction

Flame development, efficiency and emissions of a gasoline direct injection engine are strongly related with mixture preparation as reported at, Van Overbrüggen et al. (2012), Huang et al. (2008), Justham et al. (2006), Stansfield et al. (2007), Khalighi (1991). To promote sustainability and reduce emissions of greenhouse gases, future fuels are anticipated to contain significant quantities of biological components (alcohols), Williams et al. (2014), because of their production methods that are renewable. The use of gasoline blends with alcohols will change the procedure of mixture preparation, especially when they are used in gasoline direct injection engines (GDI), as well as the procedure of ignition of the fuel mixture because different biofuels have different physical and chemical properties, Liu et al. (2007), Wu et al. (2011), Aleiferis et al. (2017). Regarding the mixing process, it is crucial to investigate the dominant structure (tumble) which is created at the plane passing through the cylinder axis of symmetry, B. Murali et al. (2015a), Dannemann et al. (2009). The tumble contains kinetic energy and when it breaks down it releases the energy to the gas for mixing, Dannemann et al. (2009), Huang et al. (2008). Previous published research papers investigate only the tumble plane Khalighi (1991), Justham et al. (2006), Stansfield et al. (2007). In the current work the flow field was studied at two different planes, in order to better investigate the 3D phenomena taking place in a GDI engine. The velocity vectors were calculated at the intake stroke for 25% throttle opening corresponding to 500mbar intake pressure. The turbulent kinetic energy (TKE) and the tumble ratio (TR) were calculated based on the instantaneous 2D vector fields. The purpose of this process was the characterization of the flow field and, this was the first step of a more general

research plan to investigate mixing process with different fuel blends and see how they affect combustion process.

2. Experimental procedure

2.1. Experimental setup

A Spark Ignition (SI) Single Cylinder Optical Research Engine, manufactured by AVL, with transparent cylinder and piston crown (Figure 1) was employed for these measurements. The engine has a pent-roof shaped combustion chamber and its specifications are listed in Table 1.

Displaced volume	475 cc
Stroke	90 mm
Bore	82 mm
Connecting Rod	144 mm
Compression ratio	9.68:1
Engine speed	1000 and 1500
Number of Valves	4
Intake valve diameter	33.89 mm
Exhaust valve	28 mm
Intake valve lift	10.54 mm at 260 BTDC
Exhaust valve lift	9.18 mm
Inlet Valve Open	370° BTDC of Combustion
Inlet Valve Close	140° BTDC of Combustion
Exhaust Valve Open	585° BTDC of Combustion

Table 1: Engine specifications

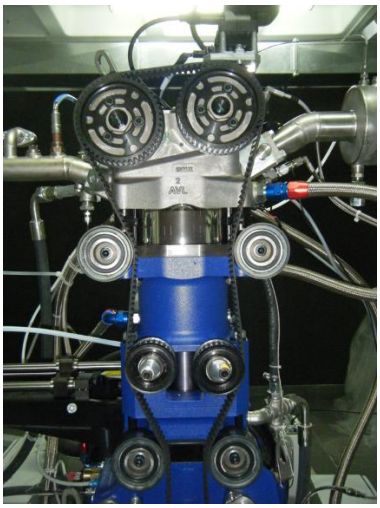

Figure 1: AVL Engine

The 475cc SI engine has two intake and two exhaust valves. The piston head and conrod are connected with an extension which allows the reflection of the laser light sheet, through a 45^0 mirror, into the engine combustion chamber. The engine was driven by a 30KW DSG dynamometer.

2.2. Low-repetition rate PIV Method

The PIV system consisted of a 10 Hz single pulse Nd:YAG laser (Continuum Surelite III 10), equipped with a double pulse option (DPO) device, with maximum power of 446mJ per pulse at 532nm. Scattering light of tracer particles was captured by a PIV camera (LaVision imager Pro X2M) with a 50mm, f#1.8 Nikon lens. Corn oil droplets of 0.9 μm mean diameter, appropriate for cold flow engine measurements as presented at Melling (1997), seeded the flow through a PIVTEC oil droplets seeder. The experimental setup is illustrated in Figure 2. At tumble plane, the laser sheet is directed into the combustion chamber through the transparent piston head and the camera captures the light in front of the cylinder.

The post processing of the PIV images was conducted using the LaVision DaVis 7.2 software. The PIV images were cross-correlated with decreasing window size multi-pass strategy from 128 pixels x 128 pixels to 32 pixels x 32 pixels with 75% overlap. The final 32 pixel x 32 pixel interrogation window corresponds to 1.8 x 1.8 mm^2 and vectors appear every 0.45mm, creating a 30000 vectors mesh. The minimum time interval between the two pulses was 20.5μs due to DPO limitations. The DPO is a device that separates the single pulse by using a shutter. A 3 pixels x 3 pixels Gaussian smoothing

filter was applied to remove noise at spatial scales near the resolution limit of PIV measurements, Dreizler et al. (2014). Velocity vectors were plotted using tecplot360 2013R1.

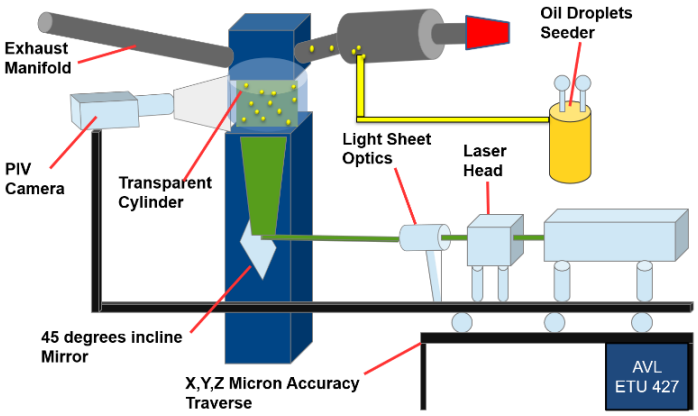

Figure 2: Schematic diagram of the experimental Setup.

To confirm that the particles had the ability to follow the flow, the particle relaxation time τ_s was calculated, Raffel et al. (2018):

$$\tau_s = d_\rho^2 \frac{\rho_p}{18\mu} \tag{1}$$

where d_ρ is the particle diameter, ρ_p is the particle density and μ is the kinematic viscosity. By using equation (1), in case of sudden deceleration, the step response of U_p typically follows the exponential law according to equation (2), Raffel et al. (2018).

$$U_p(t) = U\left[1 - exp\left(-\frac{t}{\tau_s}\right)\right] \tag{2}$$

where U_p is the particle velocity and U is the surrounding flow velocity. The ratio U_p / U can provide an estimation of how fast the particles response when the flow decelerates or accelerates. As illustrated in Figure 3, the particle velocity can reach the flow velocity in about $1.5*10^{-7}$s. This time response is acceptable for this application because the time interval between two consecutive PIV images is $20.5*10^{-6}$s. Moreover, the time scales of similar flow structures presented in the literature Aleiferis et al. (2017)are in the range of about 10^{-3}s for 1000 – 1500 RPM.

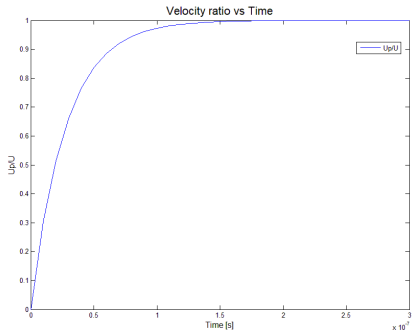

Figure 3: Particle response time.

3. Results and discussion

3.1. Velocity Measurements

Figure 4: XY plane (a) illustrates a typical raw PIV image captured at the XY plane (figure 4 (b)) when the intake valves were wide open. The red square indicates the part of field of view which is free from reflections and noise for better results illustration. This area is 66mm wide with the current setup. The red square to Bore ratio is 0.80, as presented in equation (3), and it is similar with other works presented in the literature Karhoff et al. (2013).

$$\frac{red\ square\ width}{Bore} = 0.80 \qquad (3)$$

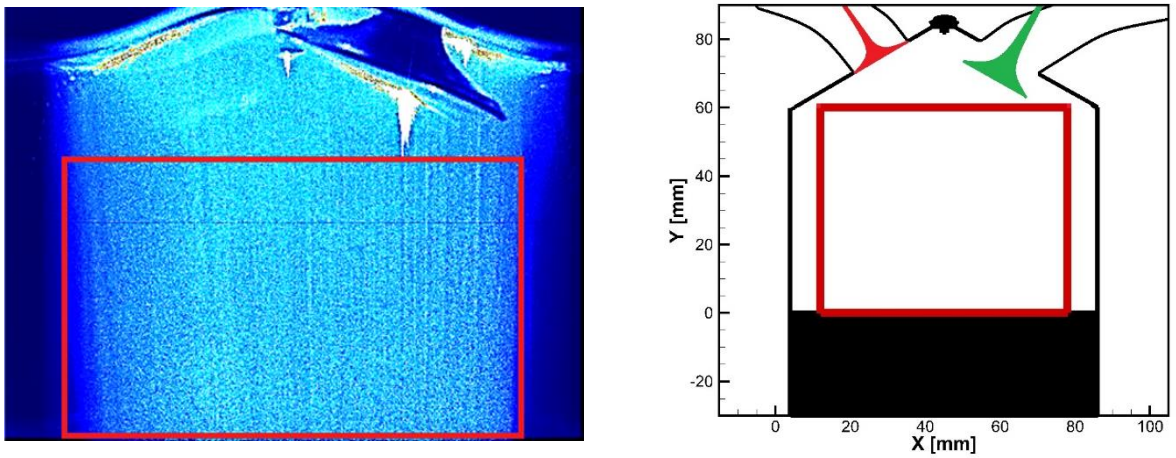

(a) Row image

(b) XY plane Schematic, green and red valve corresponds to intake and exhaust valve respectively.

Figure 4: XY plane

The other measured plane denoted by ZY, is a plane normal to the tumble plane, crossing the spark plug and separating the intake and exhaust valves.

Indicative results of ensemble averaged flow field at the intake stroke using 25% throttle opening, corresponding to intake pressure of 500mbar, are shown in Figure 5. At 300 CADs BTDC with 7.9mm valve lift, the piston moves downwards and the intake valve continues to open. It is observed that the velocity vectors magnitude at the right-hand side of the image (under the intake valve) is higher than the velocity at the left-hand side of the image. In Figure 5 (c) and (d) the intake valves are wide open (10.54mm valve lift) and the piston continues to move downwards. The main air flow steam enters from the left-hand side of the intake valves and moves downwards till it faces the piston head. The rotational motion observed is counter clock wise (CCW). This motion has also been reported in the literature, Voisine et al. (2010). In this CAD the maximum velocity was present at 1500 RPM, (Figure 5(d)), and was approximately 27m/s. Moreover, the velocity magnitude becomes higher when the engine speed increases. The tumble motion in this case, (Figure 5 (c) and (d)), is fully developed but the vortex center is located at different place, whereas at 1500 RPMs the maximum velocity is higher. This fully developed large flow structure is more stable than smaller structures and may lead to higher turbulence, B. Murali et al. (2015b). In Figure 5, (e) and (f) at 220 CADs BTDC, the intake valves

are closing and the piston still moves downwards. The maximum velocity observed at 1500 RPM (Figure 6(f)) was approximately 28m/s.

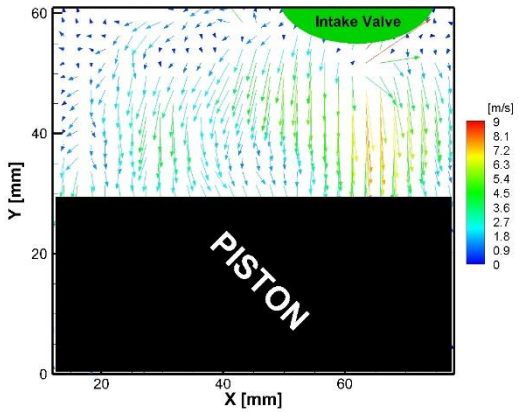

(a) 300 CADs BTDC @ 1000 RPM.

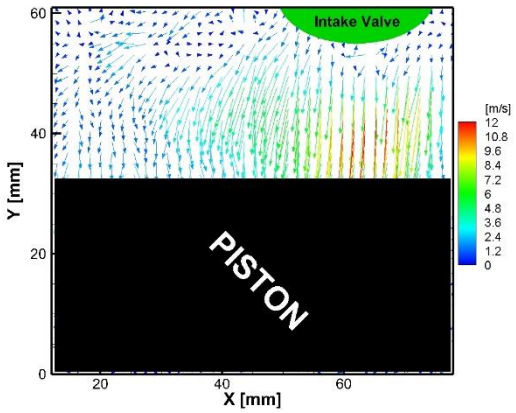

(b) 300 CADs BTDC @ 1500 RPM.

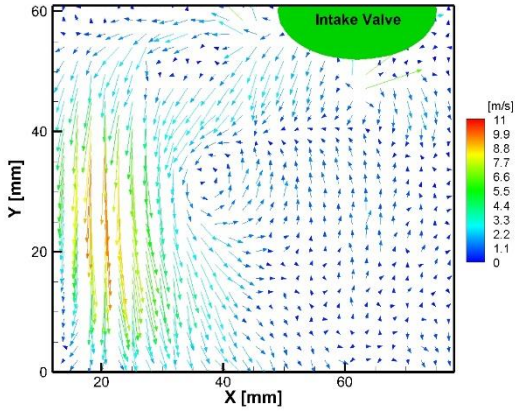

(c) 260 CADs BTDC @ 1000 RPM.

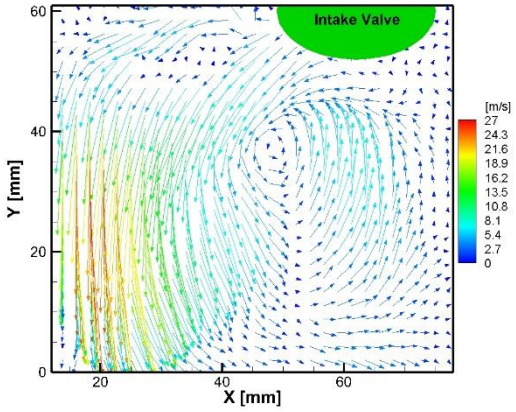

(d) 260 CADs BTDC @ 1500 RPM.

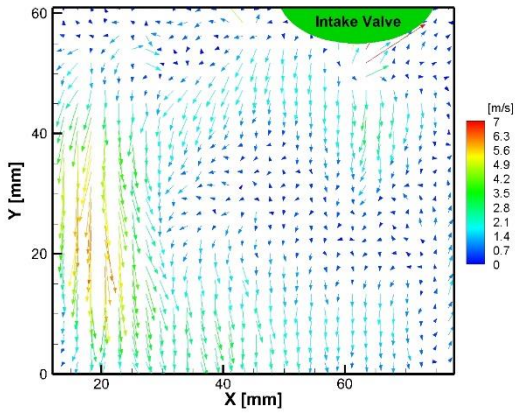

(e) 220 CADs BTDC @ 1000 RPM.

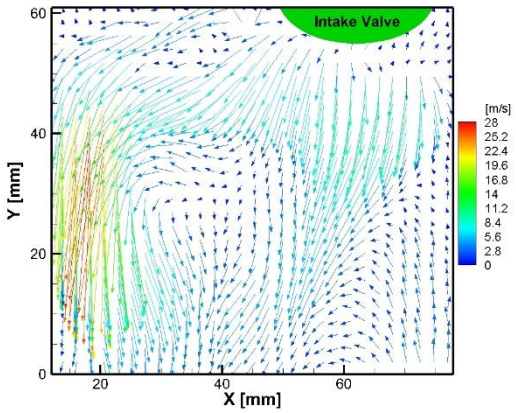

(f) 220 CADs BTDC @ 1500 RPM.

Figure 5: ZY plane with 25% throttle position and 500 mbar intake pressure.

To better understand the in-cylinder flow structures, investigation of the plane which was normal to the tumble plane was conducted. This plane (ZY plane) crosses the spark plug and separates the intake and exhaust valves, as shown in Figure 6.

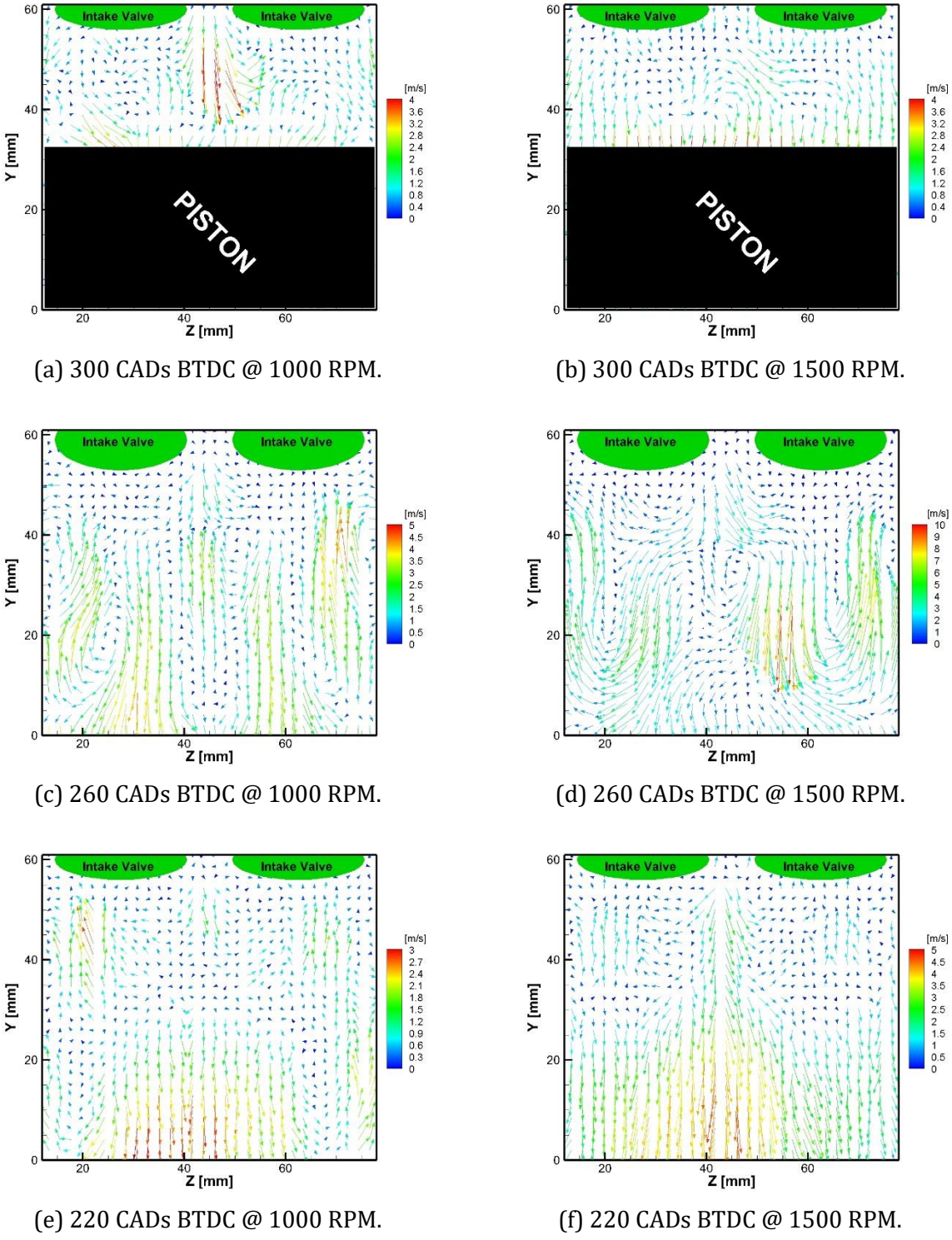

(a) 300 CADs BTDC @ 1000 RPM.

(b) 300 CADs BTDC @ 1500 RPM.

(c) 260 CADs BTDC @ 1000 RPM.

(d) 260 CADs BTDC @ 1500 RPM.

(e) 220 CADs BTDC @ 1000 RPM.

(f) 220 CADs BTDC @ 1500 RPM.

Figure 6: ZY plane with 25% throttle position and 500 mbar intake pressure.

In Figure 6, the average flow field of 2000 pair of images at 300, 260, 220 CADs BTDC at ZY plane is presented. The main flow in Figure 6 (a) and (b) was concentrated between the intake valves, moved downwards to the piston crown and then the flow reversed. At this moment the maximum velocity observed at 1000 RPM. At the 260 CAD BTDC (Figure 6 (c) and (d)) the main flow continued to move downwards between the two intake valves while the piston still moves at the same direction. At the sides of the image, the flow moves upwards against the piston motion and this motion generates small vortices. The maximum velocity at this position was observed at 1500 RPM and was approximately 10m/s. Finally, at 220 CADs BTDC, illustrated in Figure 6 (e) and (f), when the valves are nearly closed, the flow moves downwards due to the piston motion. There is a small area below the intake valves where the flow moves upwards.

3.2. TKE and TR calculation

In this section, spatial averaged results of turbulent kinetic energy (TKE) are presented. The spatial average was produced without erroneous results as presented in Figure 4: XY plane. TKE was calculated using equation (4) at every CAD in which measurements were conducted.

$$TKE = \frac{1}{2}(U_i')^2 + \frac{1}{2}(V_i')^2 + \frac{1}{4}(U_i' + V_i')^2 \quad (4)$$

where U_i' and V_i' are the values of standard deviation of the velocity component at the x and y axis respectively. Turbulence is a 3D phenomenon but the PIV technique that was employed resulted into 2D vector fields. For this reason, the standard deviation of the third component of the velocity was approximated as $\frac{1}{2}(U_i' + V_i')^2$.

The estimation of the TKE was for the XY measurement plane and not for the entire volume of the combustion chamber as the PIV method used was a 2D technique. TKE during intake stroke was found to be higher at 1000 RPM for the XY plane, presenting a maximum of 123 m^2/s^2 at 260 CAD BTDC. Moreover, the TKE at XY plane was higher than the TKE of the ZY plane for every CAD.

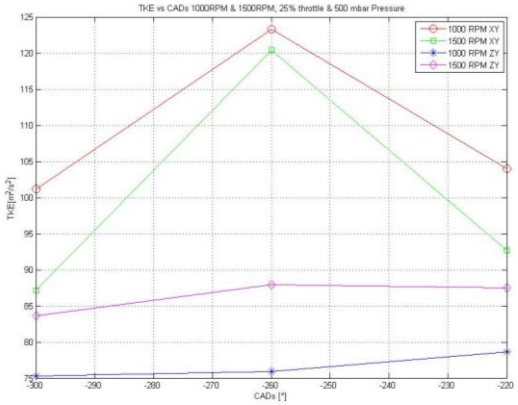

Figure 7: TKE vs CADs at 1000 and 1500 RPM with 100% and 25% throttle position, when intake valves are open.

The tumble ratio (TR) was defined as the vorticity normalized by the crankshaft angular speed as mentioned at: Stansfield et al. (2007), Huang et al. (2008), El-adawy et al. (2019). The tumble ratio was calculated for XY and ZY planes according to equations (5) and (6) respectively.

$$TR_{XX} = \frac{\sum_{i=1}^{n}\left(\frac{\partial v}{\partial X} - \frac{\partial u}{\partial Y}\right) i}{2n\omega} \quad (5)$$

$$TR_{ZZ} = \frac{\sum_{i=1}^{n}\left(\frac{\partial v}{\partial Z} - \frac{\partial w}{\partial Y}\right) i}{2n\omega} \quad (6)$$

The tumble ratio at 1500 RPM XY plane was much higher than the other three cases (Figure 8) meaning that the flow at this plane becomes more dominant as engine speed increases. At the XY plane the tumble ratio (TR) increases when the engine speed increases. Moreover, the maximum absolute TR at wide open throttle conditions (WOT) was observed at 180 CADs BTDC.

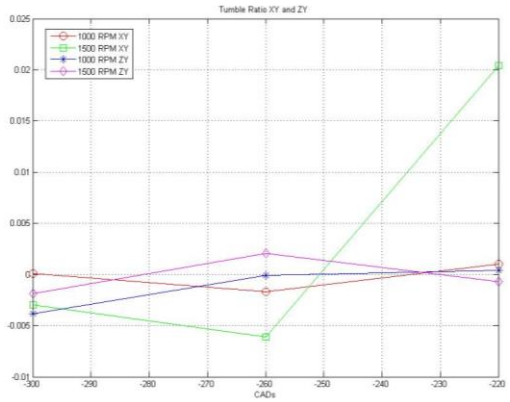

Figure 8: Tumble Ratio (TR) at XY and ZY planes.

4 Summary/ Conclusions

2D PIV technique was employed in order to characterize the flow field in a single cylinder optical research engine during the intake stroke, at 1000 and 1500 RPM engine speeds with 25% throttle opening corresponding to 500mbar intake pressure. Mean velocity field, TKE and TR of 2000 pairs of images were presented at two different planes. It was observed that:

- The maximum flow velocity at 1500 RPM is higher as compared to 1000 RPM for every CAD at tumble plane.
- A counter clock wise (CCW) tumble was present during the intake stroke at the XY plane both at 1000 and 1500 RPM.
- The maximum turbulent kinetic energy (TKE) was observed at 260 CAD BTDC for XY plane at 1000 RPM.
- TKE in every case at XY plane was found to be higher than the ZY plane.
- TR at 1500 RPM XY plane was found to be higher than in the other three cases.

Ongoing work includes measurements at more CAD positions and wide-open throttle intake pressure. Moreover, high frame rate - PIV measurements will be conducted. With these additional experimental data, it will be possible to export the time resolved characteristics of the flow and evaluate the results presented in this work. Finally, these results could form a database for evaluation of Computational Fluid Dynamic codes in multiple engine speeds, used for new engines design and development.

Acknowledgements

V.Tsiogkas is co-financed by Greece and the European Union (European Social Fund- ESF) through the Operational Programme «Human Resources Development, Education and Lifelong Learning» in the context of the project “Strengthening Human Resources Research Potential via Doctorate Research” (MIS-5000432), implemented by the State Scholarships Foundation (IKY).

D. Kolokotronis and A. Tourlidakis acknowledge support of this research work by the project “DEVELOPMENT OF THE RESEARCH INFRASTRUCTURE "CENTRE OF EXCELLENCE FOR FUTURE VEHICLE ENVIRONMENTAL PERFORMANCE"-FuVEP” (MIS 5002370) which is implemented under the Action “Reinforcement of the Research and Innovation Infrastructure”, funded by the Operational Programme "Competitiveness, Entrepreneurship and Innovation" (NSRF 2014-2020) and co-financed by Greece and the European Union (European Regional Development Fund).

References

Aleiferis, P. G., Behringer, M. K., & Malcolm, J. S. (2017). Integral Length Scales and Time Scales of Turbulence in an Optical Spark-Ignition Engine. *Flow, Turbulence and Combustion 98*(2):523–577.

Aleiferis, P. G., Behringer, M. K., OudeNijeweme, D., & Freeland, P. (2017). Insights into Stoichiometric and Lean Combustion Phenomena of Gasoline–Butanol, Gasoline–Ethanol, Iso-Octane–Butanol, and Iso-Octane–Ethanol Blends in an Optical Spark-Ignition Engine. *Combustion Science and Technology 189*(6):1013–1060.

B. Murali Krishna, & Mallikarjuna, J. M. (2015a). Effect of Manifold Inclination on an Unfired Engine Equipped with Flat Piston Using Non- Intrusive Technique – Experimental Flow Structure Analysis. *Journal of Basic and Applied Engineering Research 2*(21):1804–1809.

B. Murali Krishna, & Mallikarjuna, J. M. (2015b). PIV Experiments and In-Cylinder Flow Structure Analysis of a Motored Engine Equipped with Inclined Crown Pistons. *International Journal of Engineering Technology, Management and Applied Sciences 3*:130–139.

Dannemann, J., Pielhop, K., & Klaas, M. (2009). Cycle-Resolved Multi-Planar Particle-Image Velocimetry Measurements of the In-Cylinder Flow of a Four-Valve Combustion Engine. In *8TH INTERNATIONAL SYMPOSIUMON PARTICLE IMAGE VELOCIMETRY* - (pp. 2–5). Melbourne, Victoria, Australia.

Dreizler, E., Baum, B., Peterson, B., & Böhm, E. (2014). On The Validation of LES Applied to Internal Combustion Engine Flows : Part 1 : Comprehensive Experimental Database. Flow, turbulence and combustion 92:269–297.

El-adawy, M., Heikal, M. R., & Aziz, A. R. A. (2019). Experimental Investigation of the In-Cylinder Tumble Motion inside GDI Cylinder at Different Planes under Steady-State Condition using Stereoscopic-PIV. *Journal of Applied Fluid Mechanics 12*(1):41–49.

Huang, R. F., Yang, H. S., & Yeh, C. N. (2008). In-cylinder flows of a motored four-stroke engine with flat-crown and slightly concave-crown pistons. *Experimental Thermal and Fluid*

Science 32(5):1156–1167.

Justham, T., Jarvis, S., Clarke, A., Garner, C. P., Hargrave, G. K., & Halliwell, N. a. (2006). Simultaneous Study of Intake and In-Cylinder IC Engine Flow Fields to Provide an Insight into Intake Induced Cyclic Variations. *Journal of Physics, Conference Series 45*:146–153.

Karhoff, D., Bücker, I., Klaas, M., & Schröder, W. (2013). Time-Resolved stereoscopic PIV measurements of cyclic variations in an internal combustion engine. *10TH Internationnal Symposium on Particle Image Velocimetry -PIV13*.

Khalighi, B. (1991). Study of the intake tumble motion by flow visualization and particle tracking velocimetry. *Experiments in Fluids 10*:230–236.

Liu, S., Clemente, E. R. C., Hu, T., & Wei, Y. (2007). Study of spark ignition engine fueled with methanol/gasoline fuel blends. *Applied Thermal Engineering 27:*1904–1910.

Melling, A. (1997). Tracer particles and seeding for particle image velocimetry. *Measurement Science and Technology 8:*1406–1416.

Raffel, M., Willert, C. E., Scarano, F., Kähler, C. J., Wereley, S. T., & Kompenhans, J. (2018). *Particle Image Velocimetry, A Practical Guide, Third Edition*. Springer.

Stansfield, P., Wigley, G., Justham, T., Catto, J., & Pitcher, G. (2007). PIV analysis of in-cylinder flow structures over a range of realistic engine speeds. *Experiments in Fluids 43*(1):135–146.

Van Overbrüggen, T., Dannemann, J., Klaas, M., & Schröder, W. (2012). Holographic particle image velocimetry measurements in a four-valve combustion engine. *Experiments in Fluids 55*(1):1634.

Voisine, M., Thomas, L., Borée, J., & Rey, P. (2010). Structure and in-cycle evolution of an in-cylinder tumbling flow. *14th Int Symp on Applications of Laser Techniques to Fluid Mechanics Lisbon, Portugal*, (Elsinga 2006):05–08.

Williams, B., Edwards, M., Stone, R., Williams, J., & Ewart, P. (2014). High precision in-cylinder gas thermometry using Laser Induced Gratings: Quantitative measurement of evaporative cooling with gasoline/alcohol blends in a GDI optical engine. *Combustion and Flame 161*(1):270–279.

Wu, X., Daniel, R., Tian, G., Xu, H., Huang, Z., & Richardson, D. (2011). Dual-injection: The flexible, bi-fuel concept for spark-ignition engines fuelled with various gasoline and biofuel blends. *Applied Energy 88*(7):2305–2314.